Rare Metal Materials and Engineering
Volume 54, Issue 3, March 2025
Available online at www.rmme.ac.cn

Science Press

Cite this article as: Liang Xunwen, Fu Zhongxue, Zhang Shiming, et al. Hot Isostatic Pressing for Enhancing Mechanical Properties of Mo Alloys Prepared by Laser Powder Bed Fusion[J]. Rare Metal Materials and Engineering, 2025, 54(03): 587-592. DOI: https://doi.org/10.12442/j.issn.1002-185X.20240583.

ARTICLE

Hot Isostatic Pressing for Enhancing Mechanical Properties of Mo Alloys Prepared by Laser Powder Bed Fusion

Liang Xunwen[1,2], Fu Zhongxue[3], Zhang Shiming[4], Che Yusi[4], Cheng Pengming[5], Wang Pei[1,2]

[1] Institute of Carbon Matrix Composites, Henan Academy of Sciences, Zhengzhou 450046, China; [2] Additive Manufacturing Institute, Shenzhen University, Shenzhen 518060, China; [3] College of Mechatronics and Control Engineering, Shenzhen University, Shenzhen 518060, China; [4] Zhongyuan Critical Metals Laboratory, Zhengzhou University, Zhengzhou 450001, China; [5] State Key Laboratory for Mechanical Behavior of Materials, Xi`an Jiaotong University, Xi`an 710049, China

Abstract: To enhance the mechanical properties of Mo alloys prepared through laser powder bed fusion (LPBF), a hot isostatic pressing (HIP) treatment was used. Results show that following HIP treatment, the porosity decreases from 0.27% to 0.22%, enabling the elements Mo and Ti to diffuse fully and to distribute more uniformly, and to forming a substantial number of low-angle grain boundaries. The tensile strength soars from 286±32 MPa to 598±22 MPa, while the elongation increases from 0.08%±0.02% to 0.18%±0.02%, without notable alterations in grain morphology during the tensile deformation. HIP treatment eliminates the molten pool boundaries, which are the primary source for premature failure in LPBFed Mo alloys. Consequently, HIP treatment emerges as a novel and effective approach for strengthening the mechanical properties of LPBFed Mo alloys, offering a fresh perspective on producing high-performance Mo-based alloys.

Key words: Mo alloys; hot isostatic pressing; laser powder bed fusion; mechanical properties

1 Introduction

Molybdenum, distinguished by its remarkable properties encompassing a high melting point, low thermal expansion coefficient, and exceptional electrical and thermal conductivity, is widely employed in industries that necessitate high-temperature stability, particularly in the aerospace, energy, and electronics sectors[1–2]. In these fields, Mo alloy components are expected to possess robust mechanical properties and intricate, precise shapes, such as turbine blades, photovoltaic panel electrodes, and electronic packaging devices[3]. However, molybdenum with high melting point, low recrystallization temperature and brittleness at room temperature poses challenges during conventional casting and forging processes, while the production of intricate and precise components through traditional manufacturing methods necessitates significant costs[4].

Laser powder bed fusion (LPBF), rooted in additive manufacturing, has high flexibility and efficiency, enabling the production of intricate and precision-engineered components[5–6]. However, due to the inherent brittleness and weak grain boundary strength of Mo alloys, they are prone to cracking during rapid cooling process of LPBF[7]. Additionally, insufficient laser energy during LPBF can result in unmelted pores[8]. The thermal variation within the molten pool gives rise to surface tension gradients, triggering Marangoni convection, which hinders gas escape and leads to the creation of keyholes[9]. These defects adversely impact the mechanical properties[10–11], whereas there are some ways to reduce or eliminate them. Higashi et al[12] discovered that adjusting the volumetric energy density of laser through modifying process parameters can eliminate larger unmelted

Received date: September 04, 2024
Foundation item: National Natural Science Foundation of China (52105385); Stable Support Plan Program of Shenzhen Natural Science Fund (20220810132537001); Guangdong Basic and Applied Basic Research Foundation (2022A1515010781); Joint Fund of Henan Province Science and Technology R&D Program (225200810002); Fundamental Research Funds of Henan Academy of Sciences (240621041)
Corresponding author: Wang Pei, Ph. D., Professor, Institute of Carbon Matrix Composites, Henan Academy of Sciences, Zhengzhou 450046, P. R. China, E-mail: wangpei@hnas.ac.cn

pores in LPBFed Mo alloys, yet keyholes are invariably formed. Zhang et al[13] successfully prepared crack-free LPBFed Mo alloys by introducing Ti particles as reinforcing agents without elaborating on the presence or absence of pores. However, our subsequent test found that the LPBFed Mo alloys prepared with optimal process parameters (with element Ti added) eliminated cracks, but their tensile strength was only 286±32 MPa, far lower than that of commercial-purity (CP) Mo (534 MPa) [1], which would limit the application range of the alloys. Consequently, the porosity and strategies for further enhancing the toughness of LPBFed Mo alloys need to be investigated.

Hot isostatic pressing (HIP) treatment can serve as an effective post-treatment for LPBF due to its ability to reduce defects generated during the process without altering the shape of the components[14–15]. The elevated temperature and pressurized conditions in HIP treatment are capable of reducing the porosity of LPBFed alloys[16], improving the uniformity of their microstructures[17], and releasing their internal stresses[18], all of which have beneficial effects on the mechanical properties. However, limited reports exist regarding the application of HIP treatment to LPBFed Mo alloys. Guan et al[19] only demonstrated that HIP treatment could reduce the porosity of LPBFed Mo-La_2O_3 alloys but did not investigated other changes. The changes in microstructural features and mechanical behavior of LPBFed Mo alloys resulting from HIP treatment remain unclear and require further research.

Therefore, this work investigated the HIP treatment applied to LPBFed Mo alloys to elucidate its influence on the microstructural characteristics and mechanical performance of alloys by comparing them with the initial (as-built) samples, thereby exploring the feasibility of HIP treatment in enhancing mechanical performance of LPBFed Mo alloys.

2 Experiment

Since the addition of 2vol% Ti can eliminate cracks in LPBFed Mo alloys[13], Mo powder (D_{50}=32.9 μm) containing 2vol% of Ti particles (2−10 μm) was thoroughly mixed utilizing mechanical agitation at 80 r/min for 3 h (TURBULA T2F). Rectangular samples (5 mm×5 mm×10 mm) after polishing for microstructural characterization and tensile test samples were prepared by SLM Solutions 125 system (hatch spacing of 80 μm, layer thickness of 30 μm, scanning speed of 350 mm/s, laser power of 200 W, layer rotation angle of 90°, and continuous single-thread scanning) under the protection of 99.99vol% pure argon gas. HIP treatment was performed at 1373 K and 148 MPa with argon as the pressurizing medium, and maintained for 2 h.

The micro-surface morphology was examined by optical microscope (OM, VHX-5000), the phase identification was determined by X-ray diffraction (XRD, Empyrean, Cu-Kα), and elemental distribution was studied with electron probe microanalyzer (EPMA, SHIMADZU 8050 G). Both OM and XRD were performed along building direction (BD). In-situ room-temperature electron backscatter diffraction (EBSD) tensile tests were executed on a scanning electron microscope (SEM, GeminiSEM 360) equipped with a tensile stage (MINI-STS 2000). The EBSD detector was Symmetry S3, tensile speed was 0.001 mm/s, and no fewer than four tensile samples were measured for each type. The porosity was statistically calculated as the average value from six randomly selected OM images of the samples using Image-Pro Plus software. The geometrically necessary dislocation (GND), average grain size, and the low-angle grain boundaries (LAGBs, 2°−15°), as well as the high-angle grain boundaries (HAGBs, >15°), were analyzed using OIM Analysis software.

3 Results and Discussion

Fig. 1a and 1b reveal the surface morphologies of the as-built and HIP samples with their normalized XRD patterns, respectively. Despite the HIP treatment, pores persist with a slight reduction in porosity from 0.27% to 0.22%, which could potentially contribute to the enhancement of mechanical properties. Notably, the pores in both samples are small in size (with diameters not exceeding 10 μm) and tend to be spherical, which are generally categorized as keyholes[20]. Keyholes with a porosity less than 1% have relatively minor detrimental consequences for mechanical behavior[21]. Subsequent to HIP treatment, only the Mo (body-centered cubic) phase still exists, with the diffraction angle of the dominant (110) peak decreasing from 40.460° to 40.257°. The increase in lattice constant from 0.31503 nm to 0.31655 nm is calculated through Bragg's equation, which is likely due to variations in internal stress. The intensities of the (200) and (211) peaks are markedly weakened in the HIP samples, suggesting a shift in the direction of grain growth.

Fig.1c and Fig.1d present the SEM images and EPMA maps of as-built and HIP samples, respectively. The distribution of elements Mo and Ti in the as-built samples is uneven, and undiffused residual element Ti is observed. The higher number of red pixels representing Mo elements in Region 1, the higher content of element Mo in this area. While the corresponding content of element Ti is relatively low. The high cooling rate during the LPBF process does not allow sufficient time for Ti atoms to diffuse thoroughly within the Mo matrix[22]. Additionally, pronounced temperature gradient of the molten pool leads to varying diffusion rates of Mo and Ti atoms, engendering an uneven distribution of elements Mo and Ti. In contrast, the elements Mo and Ti in the HIP samples appear more uniform overall than those in the as-built samples, and no residual element Ti is detected. This stems from the intense heat and pressure created by HIP treatment, which provides sufficient driving force for the complete diffusion of Mo and Ti atoms. This improved uniformity of matrix (Mo) and solute (Ti) elements distribution in LPBFed Mo alloys is expected to positively impact the mechanical properties[23].

Fig. 2 displays EBSD results of the as-built and HIP samples. After HIP treatment, the average diameter of grains reduces from 58.7 μm to 45.0 μm, accompanied by a change in texture orientation, indicating the occurrence of recrystallization. Moreover, HIP treatment significantly

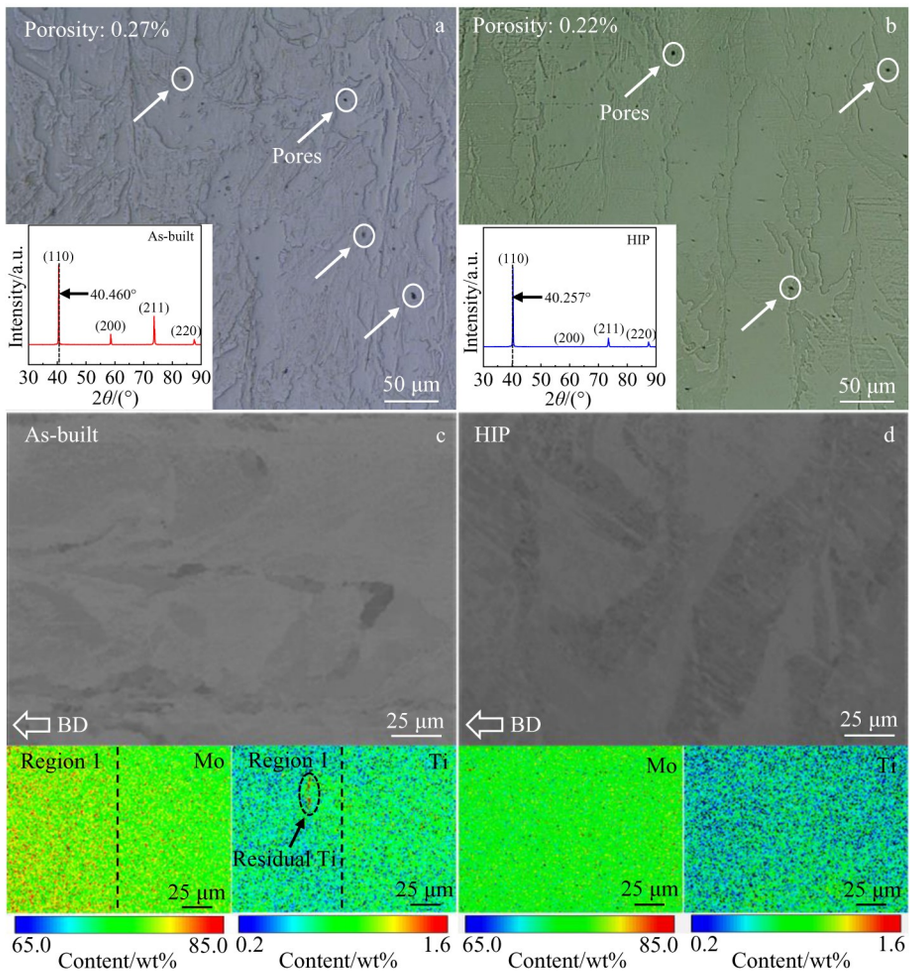

Fig.1 OM images (insets show XRD patterns) of as-built (a) and HIP (b) samples; SEM images and EPMA elemental maps of as-built (c) and HIP (d) samples

increases the fraction of LAGBs (f_{LAGBs}) from 51.7% to 84.5% and raises the average GND density from $21.99\times10^{12}/m^2$ to $46.70\times10^{12}/m^2$. On the one hand, the rapid cooling speeds and pronounced temperature differentials occur throughout the LPBF process, generating substantial lattice distortion energy within the grains[24]. Under the sustained high temperature of 1373 K during HIP treatment, this distortion energy facilitates the progression of recovery and recrystallization, promoting the rearrangement of dislocations to form LAGBs[25]. On the other hand, the HIP treatment applies a high pressure (148 MPa) to the LPBFed Mo alloys, which, in conjunction with the high temperature, increases the internal energy of the alloys, leading to the creation of a significant quantity of LAGBs in the HIP samples. The increase in GND density is primarily attributed to the elevation of f_{LAGBs}. The high f_{LAGBs} in recrystallized Mo alloys facilitates the transmission of dislocations within the grains and relieves accumulated internal stresses[26], thereby delaying the fracture of Mo alloys. The high f_{LAGBs} also has a LAGB strengthening effect on the alloys[27] and exerts a certain hindrance on crack propagation[28]. In the as-built samples, straight molten pool boundaries (MPBs) composed of HAGBs separate the grains of adjacent molten pools, whereas in HIP samples, recrystallization results in the near disappearance of MPBs.

Fig. 3a summarizes the comparison of tensile properties between as-built and HIP samples, with the tensile stress direction parallel to BD. Both tensile curves exhibit no distinct yield phenomenon, indicating that they have typical characteristics of brittle alloy. As-built samples have a tensile strength of 286±32 MPa and elongation of 0.08%±0.02%. After HIP treatment, the tensile strength and elongation elevate to 598±22 MPa and 0.18%±0.02%, representing enhancements of 109% and 125%, respectively. Notably, the tensile strength surpasses that of CP-Mo (534 MPa) as reported in Ref. [1]. The slope of the tensile curve decreases after HIP treatment. Fig.1d indicates that no residual , element Ti is found after HIP treatment. This suggests that more element Ti has been solid-solved into the LPBFed Mo alloys. Because the elastic modulus of Ti alloys is lower than that of Mo alloys, adding more element Ti may lead to a decrease in the elastic modulus of the LPBFed Mo alloys.

To gain insights into the grain evolution during the tension of HIP samples, in-situ EBSD tensile testing was performed. As depicted in Fig.3b, during tension, the f_{LAGBs}, GND density,

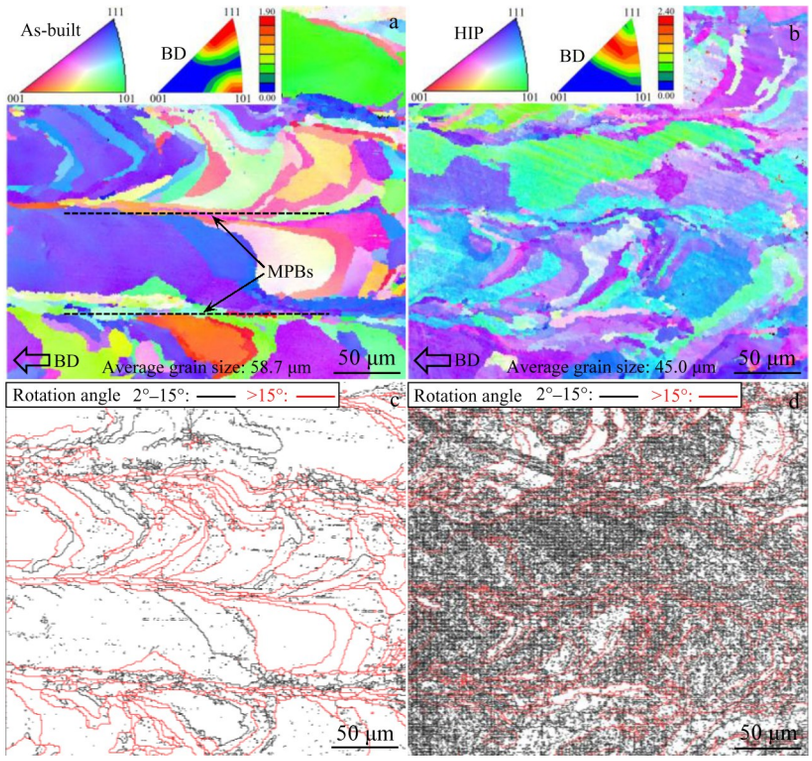

Fig.2 EBSD inverse pole figure maps (a–b) and corresponding grain boundary images (c–d) of as-built (a, c) and HIP samples (b, d)

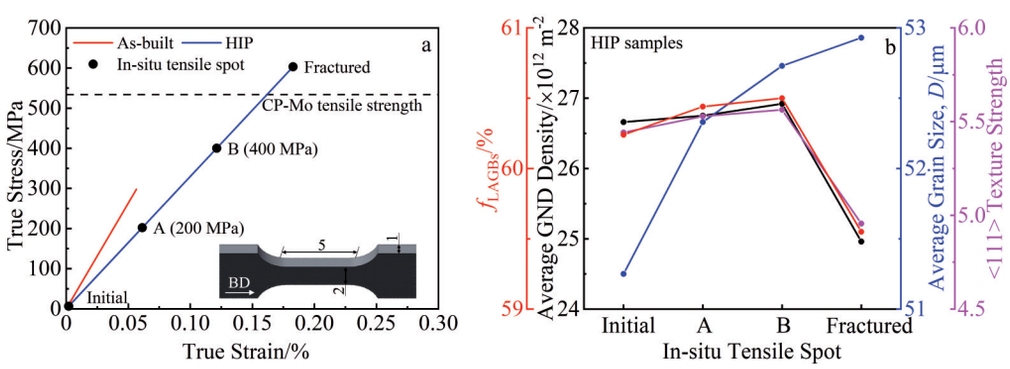

Fig.3 True stress-true strain curves of as-built and HIP samples (inset shows a diagram of plate tensile sample) (a); in-situ EBSD tensile test results of HIP samples (b)

grain size, and <111> texture strength of HIP samples all increase with stress. The grains are elongated and rotated under the application of external forces. The variation in GND density is generally governed by the amount of strain, as higher strain levels tend to increase GND density. The movement of dislocations is hindered by solute atoms (Ti) and HAGBs, leading to the formation of LAGBs, while the rearrangement of dislocation walls within grains further contributes to their formation[29]. Upon fracture, the release of stress results in a decrease in f_{LAGBs}, GND density, and <111> texture strength. However, due to the still relatively poor plasticity of the HIP-treated LPBFed Mo alloys, the grains undergo no significant changes during the tensile process.

To elucidate the causes of failure in as-built and HIP samples, their tensile fracture surfaces were investigated, as illustrated in Fig. 4. Both as-built and HIP samples exhibit typical cleavage fracture surfaces, indicating brittle intergranular fracture. The fracture surface of as-built samples is relatively flat, with crack propagation parallel to the laser scanning trajectory during the LPBF process. The corners of the crack propagation paths are nearly 90°, which align with the layer rotation angle in LPBF, and the height differences on both sides of these corners are close to the layer thickness (30 μm) in LPBF, suggesting that cracks likely propagate along the MPBs. During the LPBF process, the post-solidified regions thermally affect the already solidified regions, leading to recrystallization embrittlement of Mo alloys near the MPBs[30–31], degrading their properties and making them prone to crack initiation sites. Wen et al[32] suggested that in addition to thermal effects, sharp angle areas formed by adjacent MPBs within the same layer can also render MPBs vulnerable to crack initiation. Because the MPBs in as-built samples consist

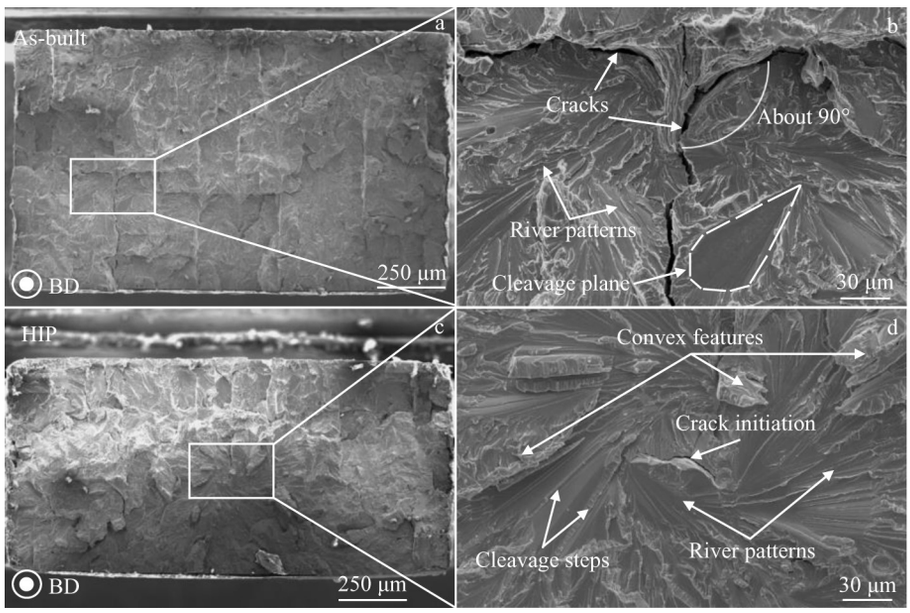

Fig.4 Tensile fracture morphologies and corresponding magnified photographs of as-built (a–b) and HIP samples (c–d)

of HAGBs oriented in a single direction, nearly along the tensile direction, as illustrated in Fig. 2a, they may offer limited resistance to crack propagation in that direction, allowing cracks to preferentially propagate along the MPBs under external forces.

In contrast, the main crack initiation in the fracture surface of HIP samples is located in centrally raised areas, and the direction of the river patterns reflects the crack propagation direction. There are numerous convex features, which to some extent increase the path and complexity of crack propagation. This is likely related to the high f_{LAGBs}, which can hinder crack propagation and necessitate the consumption of greater energy for the propagation process, contributing to improved tensile properties of the alloys. Due to the near-elimination of MPBs by HIP treatment, the fracture surface of HIP samples exhibits no fracture patterns along MPBs, thereby preventing premature failure of the alloys.

4 Conclusions

1) The mechanical properties of LPBFed Mo alloys through HIP treatment are improved. The elevated temperature and intense pressure generated by HIP treatment reduce the porosity of the LPBFed Mo alloys from 0.27% to 0.22%, leading to a more uniform distribution of elements Mo and Ti. Additionally, recrystallization occurs, resulting in the almost complete disappearance of MPBs. The f_{LAGBs} increases significantly from 51.7% to 84.5%, which not only introduces LAGB strengthening but also blocks crack propagation. The tensile strength of the LPBFed Mo alloys escalates from 286±32 MPa to 598±22 MPa, and the elongation improves from 0.08%±0.02% to 0.18%±0.02%. Despite these notable enhancements, the HIP samples still exhibit brittleness, with minimal grain deformation during tensile testing.

2) Fractographic analysis reveals that MPBs are prone to acting as crack initiation or propagation paths in the LPBFed Mo alloys, contributing to premature failure. Because of the small numerical difference in porosity after HIP treatment, the reduction in porosity may exert a certain influence on the improvement of tensile properties. However, the more significant factors are the uniform distribution of elements Mo and Ti, the high f_{LAGBs}, and the elimination of MPBs. This work establishes the remarkable influence of HIP treatment on enhancing the mechanical characteristics of LPBFed Mo alloys, thereby preparing the ground for the advancement of LPBFed Mo alloys with high mechanical performance.

References

1 Liu G, Zhang G J, Jiang F *et al. Nature Materials*[J], 2013, 12(4): 344
2 Cockeram B V. *Metallurgical and Materials Transactions A*[J], 2009, 40(12): 2843
3 Perepezko J H. *Science*[J], 2009, 326(5956): 1068
4 Cockeram B V. *Materials Science and Engineering A*[J], 2010, 528(1): 288
5 Liu Z Y, Zhao X Y, Wu Y W *et al. Rare Metals*[J], 2022, 41(8): 2853
6 Alinejadian N, Wang P, Kollo L *et al. 3D Printing and Additive Manufacturing*[J], 2023, 10(4): 785
7 Faidel D, Jonas D, Natour G *et al. Additive Manufacturing*[J], 2015, 8: 88
8 Kang N, Li Y L, Lin X *et al. Journal of Alloys and Compounds*[J], 2019, 771: 877
9 Acharya R, Sharon J A, Staroselsky A. *Acta Materialia*[J], 2017, 124: 360
10 Li J F, Wei Z Y, Xue L F. *Rare Metal Materials and Engineering*[J], 2023, 52(8): 2783

11 Voisin T, Calta N P, Khairallah S A *et al. Materials & Design*[J], 2018, 158: 113
12 Higashi M, Ozaki T. *Materials & Design*[J], 2020, 191: 108588
13 Zhang C, Wang P, Liu C Y *et al. Journal of Alloys and Compounds*[J], 2022, 910: 164802
14 Pu Y N, Zhao D W, Liu B B *et al. Rare Metal Materials and Engineering*[J], 2024, 53(8): 2123
15 Hirata T, Kimura T, Nakamoto T. *Materials Science and Engineering A*[J], 2020, 772: 138713
16 Yan X C, Lupoi R, Wu H J *et al. Materials Letters*[J], 2019, 255: 126537
17 Kreitcberg A, Brailovski V, Turenne S. *Materials Science and Engineering A*[J], 2017, 689: 1
18 Yuan Z W, Chang F C, Chen A *et al. Materials Science and Engineering A*[J], 2022, 852: 143714
19 Guan B S, Yang X S, Tang J G *et al. International Journal of Refractory Metals and Hard Materials*[J], 2023, 112: 106123
20 Zhao C, Parab N D, Li X X *et al. Science*[J], 2020, 370(6520): 1080
21 Gong H J, Rafi K, Gu H F *et al. Materials & Design*[J], 2015, 86: 545
22 Wang J C, Liu Y J, Liang S X *et al. Journal of Materials Science & Technology*[J], 2022, 105: 1
23 Fu J, Li H, Song X *et al. Journal of Materials Science & Technology*[J], 2022, 122: 165
24 Levkulich N C, Semiatin S L, Gockel J E *et al. Additive Manufacturing*[J], 2019, 28: 475
25 Mrotzek T, Hoffmann A, Martin U. *International Journal of Refractory Metals and Hard Materials*[J], 2006, 24(4): 298
26 Chen W S, Li X Y, Jin S B *et al. Nature Communications*[J], 2023, 14(1): 8336
27 Cabibbo M. *Materials Science and Engineering A*[J], 2013, 560: 413
28 Li S C, Zhu G M, Kang Y L. *Journal of Alloys and Compounds*[J], 2016, 675: 104
29 Li S C, Guo C Y, Hao L L *et al. Materials Science and Engineering A*[J], 2019, 759: 624
30 Primig S, Leitner H, Clemens H *et al. International Journal of Refractory Metals and Hard Materials*[J], 2010, 28(6): 703
31 Yang L, Zheng X Y, Zhao Y *et al. Rare Metals*[J], 2024, 43(8): 3946
32 Wen S F, Li S, Wei Q S *et al. Journal of Materials Processing Technology*[J], 2014, 214(11): 2660

热等静压处理提升激光粉末床熔融成形钼合金的力学性能

梁迅文[1,2]，付忠学[3]，张石明[4]，车玉思[4]，程鹏明[5]，王　沛[1,2]
(1. 河南省科学院 碳基复合材料研究院，河南 郑州 450046)
(2. 深圳大学 增材制造研究所，广东 深圳 518060)
(3. 深圳大学 机电与控制工程学院，广东 深圳 518060)
(4. 郑州大学 中原关键金属实验室，河南 郑州 450001)
(5. 西安交通大学 金属材料强度国家重点实验室，陕西 西安 710049)

摘　要：为了提升激光粉末床熔融（LPBF）技术所制备的钼（Mo）合金的力学性能，采用了热等静压技术对其处理。热等静压处理后，LPBF Mo合金的孔隙率从0.27%降低至0.22%，Mo和Ti元素得到充分扩散并且分布地更加均匀，同时形成了大量低角度晶界，抗拉伸强度从286±32 MPa升高至598±22 MPa，伸长率由0.08%±0.02%提高至0.18%±0.02%，在拉伸过程中晶粒没有明显变化。热等静压处理消除了LPBF Mo合金的熔池边界，而熔池边界是LPBF Mo合金提前失效的主要原因。因此，热等静压处理成为了一种有效的强化LPBF Mo合金力学性能的方法，为制造高性能钼基合金提供了新思路。

关键词：钼合金；热等静压；激光粉末床熔融；力学性能

作者简介：梁迅文，男，1998年生，硕士，河南省科学院碳基复合材料研究院，河南 郑州 450046，E-mail：liangxunwen_szu@163.com